Nuclear Bursts Produced in the Low Energy Nucleonic Component of the Cosmic Radiations*

J. A. SIMPSON, H. W. BALDWIN,† AND R. B. URETZ

Institute for Nuclear Studies, University of Chicago, Chicago, Illinois

(Received June 11, 1951)

The production rate of low energy nuclear bursts or stars has been measured as a function of altitude and geomagnetic latitude, λ, at 0°, 40° N and 52° N through 65° N. The measurements were obtained in aircraft using fast electron collection pulse chambers. Exponential absorption paths, $L_b(\lambda)$, for the nuclear burst or star producing radiation below $\sim$200 g-cm^{-2} are $L_b(0°) = 214\pm7$; $L_b(40°) = 174\pm6$; $L_b(\geqslant 52°) = 164\pm14$ g-cm^{-2}. At an atmospheric depth of 312 g-cm^{-2} the latitude factor of increase from 0° to 52°N is 3.11 ± 0.15 on undisturbed days. The disintegration product fast neutrons have a latitude factor of 3.30 ± 0.05 under the same conditions. Integral pulse-height distributions of nuclear bursts both at 0° and 52° are represented by $N_b = AV^{-2.5\pm0.1}$, where N_b is the number of burst pulses $>$ bias energy V.

A similar study of local showers produced in lead over the chambers at 0° and 52° shows a latitude factor of <1.1 and an exponential absorption of the shower producing radiations at all latitudes of 134 ± 7 g-cm^{-2}. The integral pulse-height distribution for showers was $N_s = BV^{-2.0\pm0.15}$.

From the measurements it is concluded that (a) the small stars are produced in atoms by inelastic collisions and knock-on processes by nucleons and the average number rather than the average energy of the stars produced by high energy nucleons increases with increasing primary nucleon energy, (b) the small nuclear bursts are in equilibrium with the fast neutron production in the atmosphere below $\sim$200 g-cm^{-2} and these small bursts account for almost the entire fast neutron intensity in the atmosphere, (c) these small stars and neutrons represent the low energy limit of the nucleonic component, (d) the production rate of small nuclear stars is not strongly dependent on primary nucleon momentum above $\sim$4 Bev/c.

I. INTRODUCTION

THE investigation discussed in this paper includes the measurement of the latitude and altitude dependence of the nuclear bursts or stars which are produced in fast pulse ion chambers. It was the purpose of the measurements to determine the extent to which the neutron distribution observed in the atmosphere[1] approximates the star production distribution, to identify the principal star producing processes which occur, and to measure the intensity and energy distribution of stars as a function of primary particle momentum.

The measurements extended over the regions of the atmosphere where the star producing radiations were expected to be in equilibrium with star production; namely, at atmospheric depths greater than $\sim$200 g-cm^{-2} which is below the air transition maximum in the atmosphere. Measurements were obtained at 0° (Lima, Peru), 40°, and 52–65° N geomagnetic latitude in B-29 type aircraft and included the period April through October, 1949.

The detectors used in the experiment were fast electron collection pulse chambers at high gas pressure which measured the energy lost by ionization in the chamber gas due to a nuclear burst in the thin wall or gas of the chamber. Nuclear burst measurements using this type of detection have been reported by Bridge, Rossi and co-workers,[2] and in general, the methods used in the present investigation are similar to those already developed by Bridge and Rossi.[2] They have reported

altitude measurements of the nuclear burst rates at $\lambda \approx 54°$ N. The recent work of McMahon, Rossi, and Burditt[3] using a chamber under 6 inches of lead has extended the measurements to 20° N; however, their apparatus required $>$0.4-Bev protons to produce a nuclear burst in the ion chamber when not associated with penetrating particles. The results to be discussed here are for a thin wall chamber with a roof of less than $\sim$1 g-cm^{-2}. The results extend the measurements of small stars already reported.[4]

Studies of the altitude dependence of stars observed in photographic emulsions are numerous and recently measurements of the latitude dependence of stars at mountain altitudes[5] or in the stratosphere[6] above the transition maximum have been made. In general, these measurements are of larger stars than those to be reported below.

II. EXPERIMENTAL EQUIPMENT AND PROCEDURES

A. Detectors

The ion chamber dimensions are: effective length$=51$ cm; cathode diameter$=7.6$ cm; center electrode $=0.0635$ cm; brass wall thickness$=0.079$ cm. The chambers were tested for small leaks using helium gas and a mass spectrometer and then filled with highly purified[7] argon to 75 pounds per square inch above

* Assisted by the joint program of the ONR and AEC.
† Deceased.
[1] J. A. Simpson, Phys. Rev. 83, 1175 (1951); Phys. Rev. 73, 1389 (1948).
[2] Bridge, Hazen, Rossi, and Williams, Phys. Rev. 74, 1083 (1948); H. Bridge and B. Rossi, Phys. Rev. 75, 810 (1949); H. Bridge and B. Rossi, Phys. Rev. 71, 379 (1947).

[3] McMahon, Rossi, and Burditt, Phys. Rev. 80, 157 (1950).
[4] J. A. Simpson and R. B. Uretz, Phys. Rev. 76, 569 (1949); Proc. Echo Lake Conf. 1949; J. A. Simpson and E. Hungerford, Phys. Rev. 77, 847 (1950).
[5] Morand, Beets, and Winand, Compt. rend. 229, 227 (1949); 231, 851 (1950); S. Lattimore, Phil. Mag. 41, 961 (1950).
[6] M. Schein and J. J. Lord, Phys. Rev. 73, 189 (1948); Salant, Hornbostel, Fisk, and Smith, Phys. Rev. 79, 184 (1950); J. J. Lord, Phys. Rev. 81, 901 (1951) and references therein.
[7] The following procedure was followed in preparing the argon gas for use in the electron collection chamber: 1. The gas was
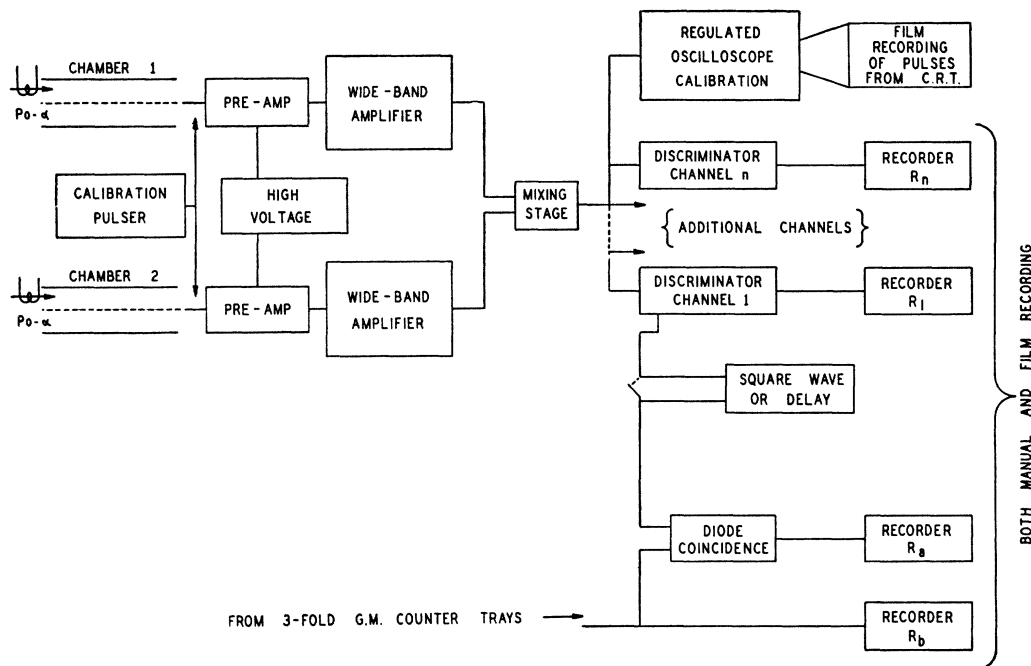
FIG. 1. Block diagram of electronic circuits used to measure the frequency and energy loss distribution of nuclear bursts or stars in fast electron collection ion chambers. There was provision for recording air and local showers using three trays of G-M counters distributed over an area which included the pulse ion chambers.

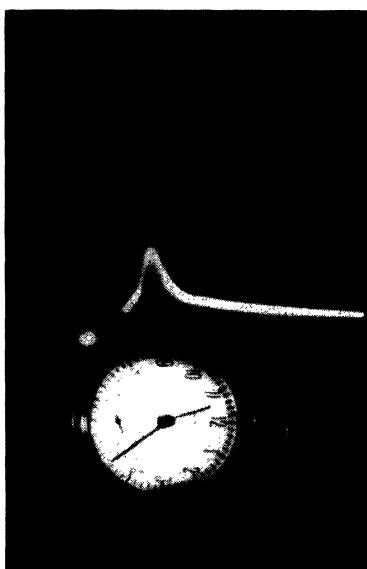vacuum pressure. The cathodes were operated at ground potential. Each chamber contained a retractable thin

FIG. 2. Calibration point on the continuous motion film recording of oscillograph traces. In the above picture the film transport has been stopped and the thin polonium source has been injected into the chamber volume. The image of the clock appears in 5-minute intervals on the film. The calibration grid is from an edge illuminated Lucite screen and is used only during calibration.

dried at liquid N_2 temperature. 2. The gas was bubbled through liquid lithium at approximately 300°C. 3. The remaining impurities: a. $O_2+H_2+CO_2$ total less than 5 ppm. b. N_2 was less than 7 ppm. 4. The baked and vacuum tested chambers were filled with the argon.

polonium alpha-particle source which could be inserted in the sensitive counting volume by energizing an external solenoid. The alpha-particle pulses reached saturation above 450 volts applied potential and the chamber operating region extended beyond 1100 volts with a change of alpha-pulse size of less than 1 percent per 100 volts change in potential. The ion chambers were operated at 750 volts.

B. Electronic Circuits

Mounted on the end of each chamber was a wide band preamplifier with gain 30 which transferred pulses through a cathode follower to a multistage wide band amplifier. (See Fig. 1.) The system of chambers and amplifiers had a rise time of 2×10^{-7} sec and a pulse clipping time of 1.1×10^{-5} sec. Two identical systems of chambers and amplifiers were used in parallel to double the observed nuclear burst rates. The outputs from the two amplifiers were coupled to a mixing stage which, in turn, was coupled to a series of pulse-height
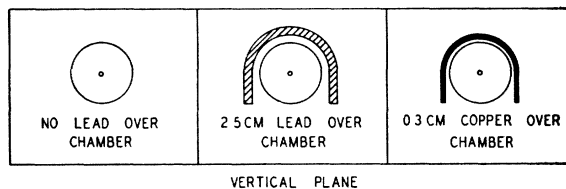

FIG. 3. These three geometries are used to separate local showers and nuclear bursts. The lead shield may be placed over the copper shield to demonstrate the negligible contribution of the lead to the nuclear burst rate in the chamber. See Sec. III(b).

TABLE I. Summary of nuclear burst and shower data obtained April–October 1949 using fast electron collection ion chambers with the geometries shown in Fig. 3. The total number of events recorded and the number of events per hour are shown for $K = V/V_{Po}$.

λ	Pressure altitude ft	Shield over chambers	K=0.8		K=1.1		K=1.1		K=1.3		K=1.5		K=2.0	
			total	c/hr	total	c/hr	total	c/hr	total	c/hr	total	c/hr	total	c/hr
0°	22,700	none							351	105±6[a]	229	75±5[a]	145	43.4±3.6[a]
	30,000	none			1029	228±7[a]			746	166±6	513	114±5		
	30,000	none			322	245±14			221	168±11	169	128±10	103	78±8
	30,000	Pb			1299	786±22			960	582±18	755	458±16	415	252±13
	35,000	none							451	220±10	352	171±9	213	104±5
40°	22,700	none			622	249±10			422	169±8	294	118±7	158	63±5
	22,700	Pb			514	482±21			361	338±18	261	242±15	143	134±11
	30,000	none			834	535±19	816	523±18	525	338±15	418	268±13	252	162±10
	30,000	none			1024	512±16			653	326±13	479	239±11		
	30,000	none	1412	1412±38	525	525±22			334	334±19			140	140±12
	30,000	Pb			1156	1156±35	1096	1096±33	769	769±28	587	587±25		
	36,000	none	2612	1741±35	1120	747±22			782	521±19			347	231±12
	36,000	none			921	700±23			693	526±20	526	399±18	278	211±13
	36,000	Pb			1717	1632±39			1268	1208±34	942	897±32	473	451±21
52° to 65°	22,700	none	1282	1148±34	442	396±19			274	246±16	198	177±18		
	30,000	none			1381[b]	621±17	1585	710±18	1036	464±15	814	364±13	566	253±11
	30,000	none			506	710±30	443[b]	625±30	335	473±27	236	334±23		
	30,000	none			1588	794±20	1520	760±20	1023	511±16			458	229±11
	30,000	none			350	712±38			234	476±32	181	368±28	92	188±20
	30,000	Pb			1182	1182±34	1216	1216±35	913	913±30	694	694±26		
	30,000	Pb			1276	1276±34	1270	1270±35	964	964±32	720	720±27	419	419±20
	30,000	Pb			1162[b]	1162±35			825	825±29	662	662±26	357	357±19
	30,000	Pb	2249	2305±48	1181	1210±35			884	806±31	641	668±27		

[a] All errors are standard statistical deviations.   [b] Bias drifted during measurement.

discriminator channels each with independent bias controls. The pulses from the amplifiers were also traced on an oscilloscope screen (with provision for inserting a delay line) and the pulse amplitude and shape was recorded on a continuous motion film camera on which the time was recorded each 5-minute interval. All mechanical registers were mounted on a panel with time, temperature and free air pressure indicators. This panel was photographed in 5-minute intervals and,

independently, each run of data was manually recorded by the operator.

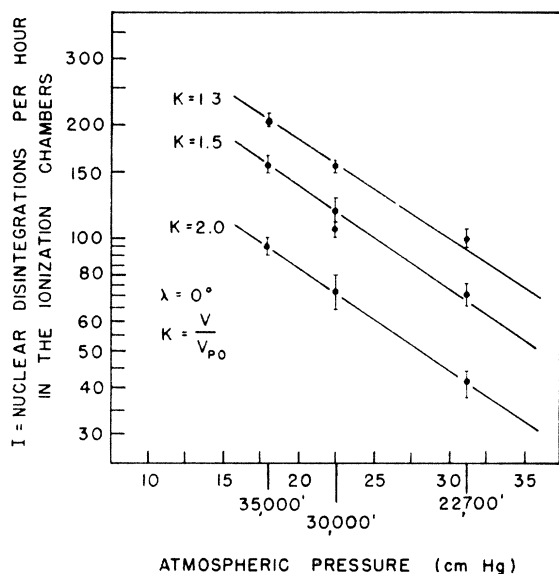The equipment operated from an electronic regulated power supply with additional electronic regulation for
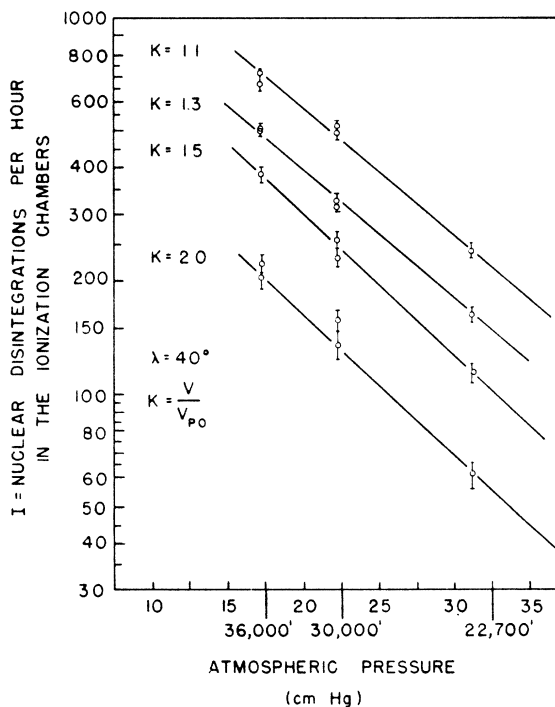

FIG. 4. The production of nuclear disintegrations in pulse ion chambers as a function of atmospheric depth at geomagnetic latitude λ=0° (Lima, Peru). The absorption $L_b(0°)$ of the nuclear burst or star producing radiation is given in Table II.

FIG. 5. The production of nuclear disintegrations in pulse ion chambers as a function of atmospheric depth at geomagnetic latitude λ=40° N. The absorption $L_b(40°)$ of the nuclear burst or star producing radiation is given in Table II.

the discriminator heater voltages, high potentials and $B+$.

C. Calibration

The pulse height at the amplifier outputs and the oscilloscope screen changed linearly with chamber pulse height within ± 2 percent from 0.5 V_{Po} to 4.0 V_{Po}, where V_{Po} is the pulse height of the polonium alpha-particle and represents an ionization loss in the argon of 5.3 Mev. The calibration procedure for each measurement was as follows: using a calibrated screen on the oscilloscope the alpha-pulse heights from the two chambers were made equal. The pulse generator which produced periodic pulses similar in shape to the alpha-pulses was then coupled to a preamplifier and used to obtain pulses of height KV_{Po} as observed on the oscilloscope screen. The discriminator bias levels were adjusted individually for any desired values of KV_{Po}. A typical calibration check during a flight is shown in Fig. 2. The entire system was recalibrated every second hour during the flights.

All burst frequency measurements which are reported below are on a relative scale.

D. Geometry

The chambers were located horizontally in the rear pressurized cabin of a B-29 with armor and radar units removed. The mass over the upper hemisphere of the chambers was <1 g-cm^{-2}. No apparatus was located under the chambers or under the floor boards of the cabin. The chambers were located 45 cm apart to avoid ionization in two chambers due to a single nuclear burst in the wall or gas of one of them. As shown by Bridge et al.[2] at mountain altitudes this effect becomes appreciable when the chambers are close together.
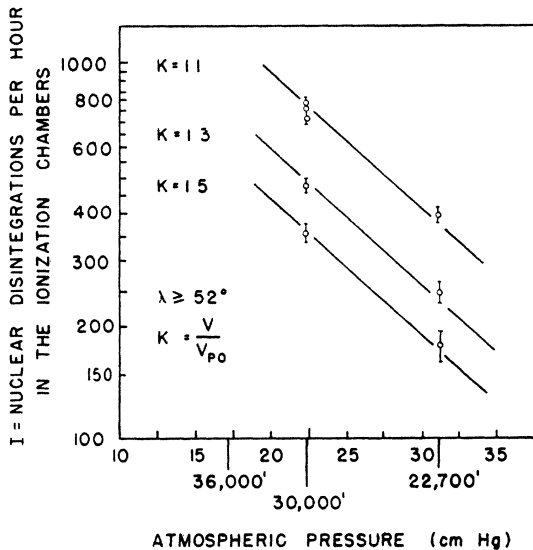
ATMOSPHERIC PRESSURE (cm Hg)

Fig. 6. The production of nuclear disintegrations as a function of atmospheric depth at geomagnetic latitude $\lambda = 52°$ N. The absorption $L_b(52°)$ of the nuclear burst or star producing radiation is given in Table II.

Table II. Exponential absorption (L_b) of the star producing radiation in the atmosphere in g-cm^{-2} air.

Lati-tude	$K = 1.1$ g-cm^{-1}	$K = 1.3$ g-cm^{-1}	$K = 1.5$ g-cm^{-1}	$K = 2.0$ g-cm^{-1}
0°		220±7	214±8	214±8
40°	174±6	174±6	160±6	160±6
52°	(164±14)	(164±14)	(164±14)	

Two basic geometries were used for the measurements to be described. The first was the unshielded chamber measurement to determine nuclear burst rate. The second geometry was the chamber covered with a hemicylinder of lead 2.5 cm thick as shown in Fig. 3.

III. EXPERIMENTAL RESULTS

The results obtained from the use of the multichannel pulse-height selector are tabulated in Table I. Flights on which serious equipment failures occurred were not included. The total number of bursts recorded, the burst frequency and standard statistical deviations are shown. Since $V_{bias} = KV_{Po}$, a range of K values was selected which would include the small burst production but be limited by background noise in the amplifiers while in flight; hence $K \geqslant 0.8$ was selected as the lowest bias and $K = 2$ was used as the highest bias. Wider ranges of burst sizes were selected from the film recording of pulse traces which will be described later.

A. Nuclear Burst Production as a Function of Altitude and Latitude

Altitude curves at 0°, 40°, and 52° are plotted in Figs. 4, 5, and 6, respectively. The experimental points appear to fit a simple exponential absorption of the burst-producing radiations of the form $I = I_0 \exp(-h/L_b)$, where h is the atmospheric depth in
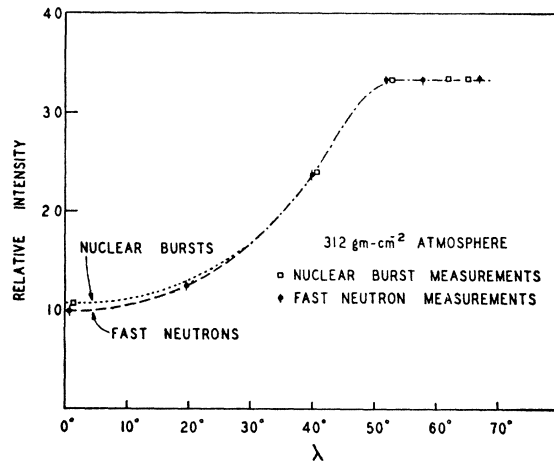
Fig. 7. The relative intensities of the fast neutron production in the atmosphere and the nuclear burst production in pulse ion chambers all at an atmospheric depth of 312 g-cm^{-2}. The curves were fitted above 52° at 3.3. It is seen that there is no evidence for an appreciable increase in nuclear burst intensity above $\lambda \approx 52°$. Neutron values plotted are for undisturbed days.
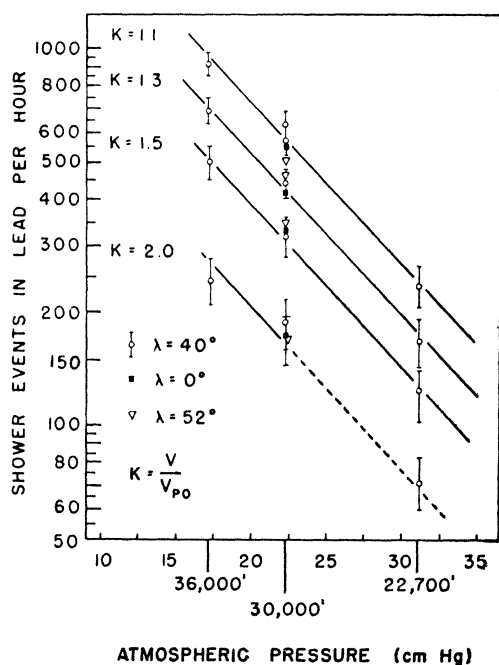
FIG. 8. The local showers produced in 2.5 cm Pb over the ion chambers has been measured as a function of atmospheric depth at $\lambda=40°$ N. Also the measurements at 312 g-cm^{-2} (30,000 ft) included $\lambda=0°$ and $\lambda=52°$.

g-cm^{-2} and L_b is the exponential absorption of the nuclear burst or star producing radiations in g-cm^{-2}. Values for $L_b(\lambda)$ have been tabulated in Table II for different latitudes and minimum bias energies KV_{Po}. The values for $L_b(52°)$ are less reliable using the two points on each curve; however, they cannot be larger than the corresponding values at $\lambda=40°$. A typical latitude curve is shown in Fig. 7.

B. Altitude and Latitude Dependence of Local Showers in Lead

In addition to the nuclear burst measurements with uncovered chembers there was a series of measurements of the local production of electronic showers in 2.5 cm of lead hemicylinders covering the chambers as shown in Fig. 3. The lead thickness was selected to coincide with the transition maximum found for local shower production in lead. The frequency of events in the lead covered chambers was due to electron showers and to the nuclear bursts as measured in III(a), since the attenuation of the nuclear burst producing radiation in 2.5 cm Pb is negligible. Hence, the difference in the measurements with and without lead gives on first approximation, the shower rate as a function of latitude and altitude. The results of these difference measurements are shown in Fig. 8.

It may be shown that the presence of lead over the ion chambers does not significantly change the production rate of *nuclear* bursts in the chambers as compared with the production rate with uncovered chambers. Consider the following sequence of four

TABLE III. The nuclear burst and shower production per hour measured at 30,000 feet pressure altitude. The geometries are shown in Fig. 3 and the interpretation of the measurements appears in Section IIIB.

	$K=0.8$	$K=1.1$	$K=1.3$	$K=2.0$
1. Uncovered chambers	1412±38	525±22	334±19	140±12
2. Copper-covered chambers	1349±34	501±20	351±17	141±11
3. 2.5 cm Pb-covered chambers	2252±45	1105±33	760±27	328±18
4. 2.5 cm Pb over copper-covered chambers	2312±19	994±32	755±28	308±18

measurements at $\lambda=40°$ as given in Table III using the geometry shown in Fig. 3.

(1) The nuclear burst rate of uncovered chambers was measured.

(2) 0.3 cm copper, in which shower production is negligible but the nuclear burst rate is not, was placed over the chambers. The chamber burst rate was, within statistics, the same as for an uncovered chamber.

(3) 2.5 cm Pb was placed over the chambers and the combined nuclear and shower rates were determined.

(4) The copper was placed over the chambers and under the 2.5 cm lead as shown in Fig. 3 to determine whether secondary nuclear burst production on the underside of the lead could contribute to the chamber counting rate.

Within statistics the results show that if any effect existed it must be negligible. Measurements described in Table IV of reference 1 also confirm this result.
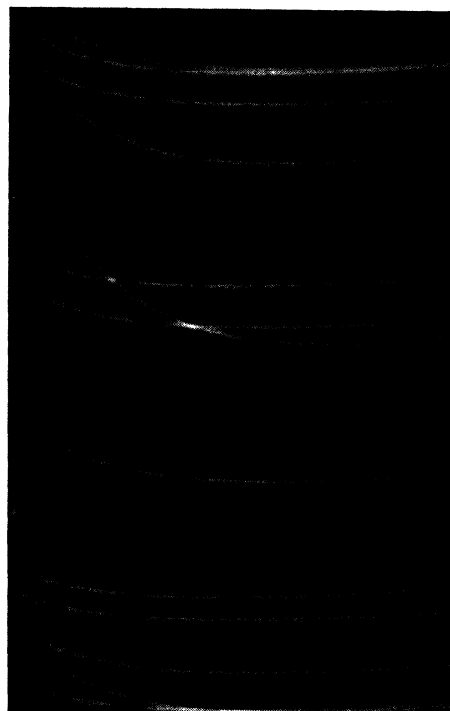

FIG. 9. A typical section of the continuous film recording of pulses. The sweep in this case was adjusted for convenient measuring of pulse height rather than rise time. The seventh pulse from the top is a typical shower event.

Further, it is evident that the events produced in lead are associated with high energy showers (≥ 13 Bev), since the shower production rate has a very small latitude dependence.

C. The Nuclear Burst Size *vs* Frequency Distribution at $\lambda = 0°$ and $\lambda = 52°$

By measuring the pulse sizes from the oscilloscope which were recorded on the continuous motion film a detailed curve of the integral burst rate as a function of bias energy has been obtained. Typical pictures of strips from the film record are shown in Fig. 9. In Fig. 10 these data are fitted on a log-log plot by straight lines. Hence, within the range of bias energies measured the burst frequency is defined by $N_b = A V^{-\gamma}$, where A is a constant, V is the pulse size in Mev, and $\gamma = 2.5 \pm 0.1$. For comparison, data obtained from Figs. 7 and 9 independently by the electronic pulse size discriminators have also been plotted.

D. The Electronic Shower Burst Size *vs* Frequency Distribution

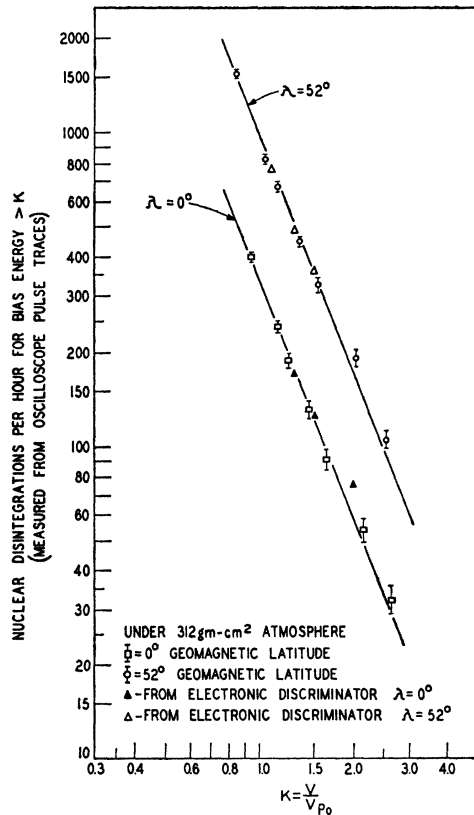With 2.5 cm Pb hemicylinders covering the chambers the pulse size distribution derived from the
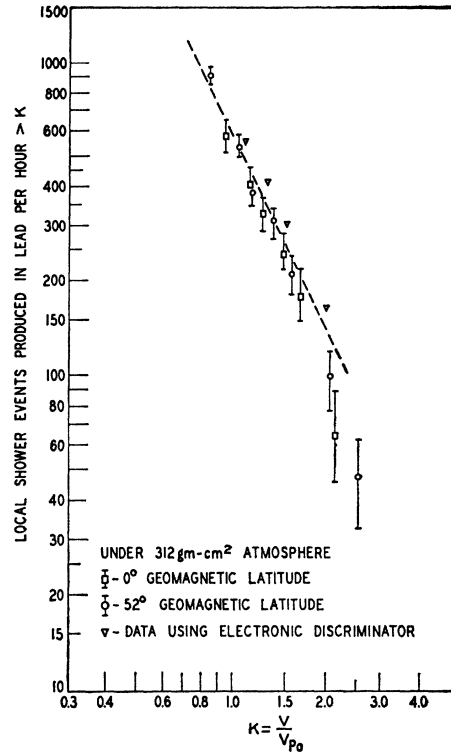

FIG. 11. The integral pulse size distribution of local showers produced in 2.5 cm Pb over the ion chambers. The points are fitted by the expression $N_s = B V^{-2.0 \pm 1.5}$.

oscillograph film recordings was obtained at 30,000 ft pressure altitude. The data for the integral shower rates as a function of K are plotted in Fig. 11. Since these data are derived from difference measurements the electron shower intensity at bias energies greater than $K \approx 1.5$ is not reliable. The slope of the curve for $K < 1.5$ is given approximately by $N_s = B V_s^{-\beta}$, where V_s is the Mev energy loss in ionization by an electronic shower and $\beta = 2.0 \pm 0.15$.

IV. DISCUSSION AND CONCLUSIONS

A. Latitude and Altitude Dependence of Star Production

It was shown by a series of measurements in Sec. IIIB that when the chambers were covered with lead, there was no observed contribution of nuclear bursts by the lead. However, air and local showers may produce measurable pulses in both the uncovered and covered chambers. Consequently, a small correction must be made to the nuclear burst data to account for the contribution of air shower events. For the measurements reported here at high altitudes this contribution was determined from the observations of pulse shapes recorded on film due to nuclear events (alpha-type pulses) and air showers (volume ionization type pulses) in the uncovered chambers. A 7 percent contribution at 30,000 ft pressure altitude and $\lambda = 0°$ was found. Since

FIG. 10. The integral pulse size distribution of nuclear bursts at $\lambda = 0°$ and $\lambda = 52°$. Both sets of data are fitted by the expression $N_b = A V^{-2.5 \pm 0.1}$. The data at 0° are corrected for shower background (Sec. IVA).

large air showers are derived from high energy primaries the frequency of these showers has negligible latitude dependence. Hence, since the latitude dependence of nuclear burst rate is ~ 3, the contribution of air showers at 52° N is ~ 2 percent. This is in agreement with the measurements of Bridge[2] and Montgomery and co-workers.[8] This correction is of importance when comparing the latitude dependence of neutrons in the atmosphere and nuclear bursts in ionization chambers. The uncorrected latitude factor for nuclear bursts under 312 g-cm^{-2} air is 2.9, but taking into account the 7 percent air shower contribution the ratio becomes $R_b = 3.11 \pm 0.15$ and is to be compared with the observed neutron production ratio of $R_n = 3.30 \pm 0.08$. The latitude effect for nuclear bursts and neutrons at 312 g-cm^{-2} is shown in Fig. 7.

The exponential absorption, L_b, is a measure of the absorption of the star or burst producing radiations in air. In order to compare at different latitudes the corresponding values L_n for fast neutrons and L_b, the values for L_b were measured by taking all nuclear bursts of size $> KV_{P_0}$, the bias energy. Using the integrated value for the nuclear burst rates is necessary, since the neutrons after being emitted from stars immediately lose their identity with stars of any given initial energy and are scattered and reduced in energy to form a neutron energy distribution distinct from the star energy distribution. At the geomagnetic equator the measured values for L_b are 214 ± 7 g-cm^{-2} with the exception of $K = 1.3$, where the L_b value was increased because of a high experimental point at 31.2 cm Hg. From reference 1 it is seen that L_b is to be compared with $L_n = 212 \pm 4$ g-cm^{-2} for fast or slow neutrons.

At $\lambda = 40°$ N the absorption L_b approaches 174 ± 6 g-cm^{-2} as the chamber bias energy is reduced. The corresponding value from fast neutron measurements in air is $L_n = 181 \pm 3$ g-cm^{-2} air.

With only two altitude points at $\lambda = 52°$ the value $L_b = 164 \pm 14$ is an approximation. It is not in disagreement, however, with the exponential absorption of the neutron producing radiation in air, $L_n = 157 \pm 2$.

The published values for L_b at $\lambda \approx 50°$ using chamber measurements are 135–150[2] g-cm^{-2} and from the stars observed in nuclear emulsions are 135[9] to 150[10] g-cm^{-2}. These values for L_b in the region of 50° tend to be lower than found in the present investigation. However, it should be noted that for the nuclear burst curves obtained at $\lambda = 0°$ and 40° fast neutron measurements were obtained concurrently in the same aircraft to confirm the earlier values for L_n; hence a systematic error in air mass determinations would have introduced a change in the L_n observed with the nuclear burst measurements if such an error existed.

The nuclear burst measurements obtained by McMahon, Rossi, and Burditt[3] under 6 inches of lead may be compared with the above measurements although their apparatus selected higher energy events. At 300 g-cm^{-2} they obtain $R_b = 1.96 \pm 0.18$ between 20° and 55° N ascribed to proton produced stars. This latitude effect is smaller than that expected from the measurements reported here (from Fig. 7 the latitude effect would be ~ 2.5 between 20° N and 52° N). This difference is most probably due to the higher energy cutoff in the experimental arrangement of McMahon. Their value for L_b at 20° is 198 ± 50 g-cm^{-2}. When extrapolated to 0° this value is consistent with the measurements reported here. Recently Whyte[11] has reported balloon flights using an unshielded spherical chamber which showed a latitude factor of approximately 3 between 0° and 52° at 312 g-cm^{-2}. Photographic nuclear emulsion measurements of small stars at mountain altitudes[6] near the geomagnetic equator and near 50° as well as measurements in the stratosphere[6] when extrapolated to the region 200–600 g-cm^{-2} atmosphere appear to be in approximate agreement with the pulse ionization chamber measurements.

B. Shower Events

The local shower events in the lead-covered chamber include both electronic and penetrating particle showers. The maximum latitude factor R_s for these events can only be estimated from Fig. 8 to be $R_s = 1.0$ to 1.1 between 0° and 52° at 312 g-cm^{-2} air. The altitude dependence of local shower production, assuming exponential dependence on atmospheric depth, is $L_s = 134 \pm 7$ g-cm^{-2}, and is in agreement with Bridge[2] and McMahon.[3] The integral shower burst spectrum, Fig. 11, is represented by $N_s = BV^{-2.0 \pm 0.15}$.

C. Energy Spectrum for Small Nuclear Bursts at $\lambda = 0°$ and 52° N

The integral small burst spectrum at 312 g-cm^{-2} has the exponent $\gamma = 2.5 \pm 0.1$ at both $\lambda = 0°$ and $\lambda = 52°$ as seen from Fig. 10. If it is assumed that nuclear bursts are produced by inelastic collisions and knock-on processes by nucleons,[1,9] it then follows from Fig. 10 that the change in average primary particle momentum between 0° and 52° produces a change in the average number of inelastic collisions rather than a change in the average energy transfer of each collision process. It is clear that production of nuclear bursts at these altitudes by fast pion capture is not prominent because of the short mean life of pions. Thus, the principal process for *small* nuclear burst production in the equilibrium region of the atmosphere appears to be a series of inelastic nucleon-nucleus collisions or knock-on collisions by a high energy nucleon with the extent of the series or chains of collisions in the atmosphere being a function of the nucleon energy. This

[8] Montgomery, Montgomery, and Northrup, Phys. Rev. 79, 293 (1950).

[9] Bernardini, Cortini, and Manfredini, Phys. Rev. 76, 1792 (1949); 79, 952 (1950).

[10] E. P. George and A. C. Jason, Cosmic Radiations, Colston Papers (Butterworths Science Publications, London, 1949).

[11] G. N. Whyte, Phys. Rev. 82, 204 (1951).

accounts for the change in exponential absorption of the star producing radiation with latitude; namely, $L_b(0°) > L_b(40°) > L_b(52°)$.

The above arguments show that the energy loss E' in a nucleon-nucleus collision producing a small star cannot be a homogeneous function of E'/E_p, where E_p is the primary particle energy. Thus, the expression $N_b = AV^{-2.5}$ for small burst production does not represent the primary energy spectrum. At much higher burst energies the measurements by Carmichael[12] and Montgomery[13] and the recent measurements in nuclear emulsions by Barton, George, and Jason[14] indicate that the large burst and star integral spectrum approaches the values for γ in the range 1.6 to 1.9.

[12] H. Carmichael, Phys. Rev. 74, 1667 (1948).
[13] C. G. Montgomery and D. D. Montgomery, Phys. Rev. 76, 1482 (1949).
[14] Barton, George, and Jason, Proc. Phys. Soc. (London) A64, 175 (1951).

The measurements described above show that the nuclear burst production and fast neutron production are substantially in equilibrium in the atmosphere below $\sim$200 g-cm^{-2}. Hence, the evidence given in reference 1 to show that the production of neutrons per primary nucleon is not strongly dependent on primary particle momentum above $\sim$4 Bev/c may be extended now to the production of small nuclear bursts in the atmosphere as a function of primary particle momentum.

The Absorption of Extensive Showers in Water*

Paul H. Barrett†

University of California, Berkeley, California

(Received July 11, 1951)

The absorption of the particles in extensive showers in water has been measured at 2765 meters elevation by detecting coincidences between trays of Geiger counters located under water. Coincidence rates have been measured with counter tray separations up to 5 meters and at seven depths from 0 to 10 meters of water. A theoretical calculation is shown to predict coincidence rates lower than those experimentally observed and further improvements in the calculations are suggested that might remove this discrepancy. If multiple cores exist in extensive showers, this experiment shows that they cannot be separated by more than 50 cm. The density spectrum and the spectrum of the number of particles in a shower have been calculated from the experimental results for elevations of 50 and 2765 meters.

I. INTRODUCTION

SINCE the discovery[1] of the extensive showers in cosmic rays by Geiger tube coincidences, many experiments have been performed to clarify the structure and composition of these showers. From the hypothesis of the cascade origin of these showers Molière[2] has calculated the electron distribution about the shower axis. These results have been shown to be in agreement with experiments performed with Geiger counters[3] and ionization chambers.[4]

A possible mechanism for the production of extensive

showers[5] predicts the presence of multiple cores. However, the hypothesis of multiple cores has been shown to be inconsistent with the results from ionization chamber[4] and counter tray[3] experiments.

Fretter and Ise[6] have reported another type of experiment to detect the presence of multiple cores. With water as an absorber the low energy particles will be absorbed. Preliminary results indicated this approach to be promising. These experiments have been extended to greater depths of water in the research reported here in an attempt to study further the structure of the shower core. Experiments were carried out during the summer of 1950 at Lake Sabrina (elevation 2765 meters) near Bishop, California. Further data were obtained in the spring of 1951 near sea level at Berkeley, California.

[1] Auger, Maze, and Grivet-Meyer, Compt. rend. 206, 1721 (1938).
[2] G. Molière, *Cosmic Radiation*, edited by W. Heisenberg (Dover Publications, New York, 1946).
[3] Cocconi, Cocconi, Tongiorgi, and Greisen, Phys. Rev. 76, 1020 (1949).
[4] R. W. Williams, Phys. Rev. 74, 1689 (1948).
[5] Lewis, Oppenheimer, and Wouthuysen, Phys. Rev. 73, 127 (1948).
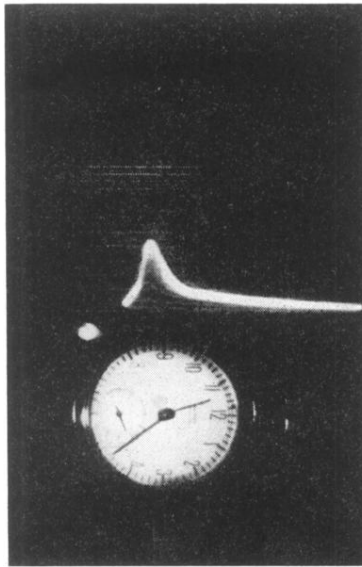[6] W. B. Fretter and J. Ise, Jr., Phys. Rev. 78, 92 (1950).

Fig. 2. Calibration point on the continuous motion film recording of oscillograph traces. In the above picture the film transport has been stopped and the thin polonium source has been injected into the chamber volume. The image of the clock appears in 5-minute intervals on the film. The calibration grid is from an edge illuminated Lucite screen and is used only during calibration.
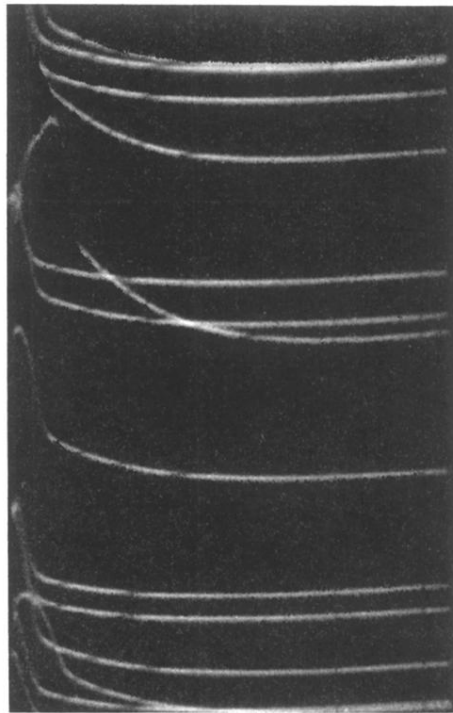
FIG. 9. A typical section of the continuous film recording of pulses. The sweep in this case was adjusted for convenient measuring of pulse height rather than rise time. The seventh pulse from the top is a typical shower event.